Spatial locality of electronic correlations in LiFeAs

Minjae Kim,[1,2,*] Hu Miao,[3] Sangkook Choi,[4] Manuel Zingl,[5] Antoine Georges,[6,5,7,8] and Gabriel Kotliar[1,4]

[1]*Department of Physics and Astronomy, Rutgers University, Piscataway, New Jersey 08854, USA*
[2]*Department of Chemistry, Pohang University of Science and Technology (POSTECH), Pohang 37673, Korea*
[3]*Materials Science and Technology Division, Oak Ridge National Laboratory, Oak Ridge, Tennessee 37831, USA*
[4]*Condensed Matter Physics and Materials Science Department, Brookhaven National Laboratory, Upton, New York 11973, USA*
[5]*Center for Computational Quantum Physics, Flatiron Institute, 162 5th Avenue, New York, New York 10010, USA*
[6]*Collège de France, 11 Place Marcelin Berthelot, 75005 Paris, France*
[7]*Centre de Physique Théorique, École Polytechnique, CNRS, Université Paris-Saclay, 91128 Palaiseau, France*
[8]*Department of Quantum Matter Physics, University of Geneva, 24 Quai Ernest-Ansermet, 1211 Geneva 4, Switzerland*

(Received 22 September 2020; accepted 19 March 2021; published 5 April 2021)

We address the question of the degree of spatial nonlocality of the self-energy in the iron-based superconductors, a subject which is receiving considerable attention. Using LiFeAs as a prototypical example, we extract the self-energy from angular-resolved photoemission spectroscopy data. We use two distinct electronic structure references: density functional theory in the local density approximation and linearized quasiparticle self-consistent GW (LQSGW). We find that with the LQSGW reference, spatially local dynamical correlations provide a consistent description of the experimental data, and account for some surprising aspects of the data such as the substantial out-of-plane dispersion of the electron Fermi surface having dominant xz/yz character. Hence, correlations effects can be separated into static nonlocal contributions well described by LQSGW and dynamical local contributions. Hall effect and resistivity data are shown to be consistent with this description.

DOI: 10.1103/PhysRevB.103.155107

I. INTRODUCTION

The origin of superconductivity in the iron pnictides and chalcogenides is an outstanding open problem in condensed matter physics [1]. Two opposite points of view have been presented. In the first one, superconductivity originates from the exchange of spatially nonlocal antiferromagnetic (AFM) spin fluctuations [2–4] and nonlocal correlations are also essential in the normal state [5–8]. The second one posits a more local pairing due to Hund's coupling [9–13], which in turn requires a rather local picture of the normal state.

Answering this question requires a proper understanding of the degree of spatial locality of electronic correlations in the normal state. This has been addressed previously by a comparison of theoretical calculations to experiments. Some results favor the local picture [14–22] while others support the nonlocal view [5,6,23–25].

Here, we take a different approach and address this question by a direct examination of experimental data from angle-resolved photoemission spectroscopy (ARPES), following the approach which was successful for Sr_2RuO_4 [26]. We consider LiFeAs [27], a prototypical iron-based superconductor which is free from magnetic and nematic instabilities and which has been intensively studied for more than a decade [7,14,18], and use the experimentally measured quasiparticle dispersions for the different Fermi surface (FS) sheets to determine the self-energy and assess its degree of spatial locality.

Our results offer a solution to the local vs nonlocal conundrum [28]. We find that the electronic self-energy can be separated, to a good approximation, into a nonlocal part which is frequency independent, and a dynamical (frequency-dependent) part which is spatially local to a good approximation. The nonlocal part can be incorporated in the reference Hamiltonian with respect to which the dynamical self-energy is defined, and we show that the quasiparticle GW approximation [29–31] provides a good starting point to that effect. These findings are in line with previous work by Tomczak *et al.* [22,29], but we emphasize that our conclusions are established directly from *experimental observations*, once the proper reference Hamiltonian to define self-energies is used. This finding rationalizes the success of dynamical mean-field theory (DMFT) [32,33] for these materials [14,34,35], and emphasizes GW+DMFT as a method of choice in this context [22,29,36].

II. METHOD

Ignoring photoemission matrix elements, extrinsic and surface effects, we relate the measured photoemission spectra to the spectral function associated with the one-particle Green's function:

$$G(k,\omega) = [\omega \cdot \mathbf{I} - H(k) - \Sigma(k,\omega)]^{-1}_{m\sigma,m'\sigma'}. \quad (1)$$

In this expression, $H(k)$ is a reference Hamiltonian matrix expressed in a localized basis of orbitals m,σ (σ is the spin index), ω is the frequency, and k is the wave vector in the Brillouin zone. $\Sigma(k,\omega)$ is the self-energy matrix for the given reference Hamiltonian $H(k)$. The chemical potential is included in $H(k)$.

*garix.minjae.kim@gmail.com

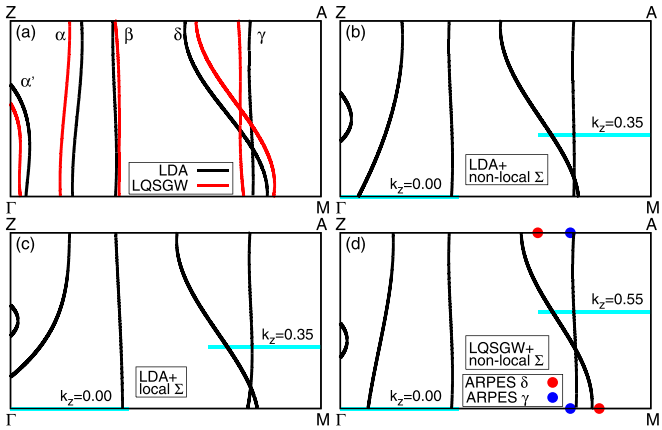

FIG. 1. (a) Fermi surfaces of LDA (black) and LQSGW (red) in the Γ-*M*-*A*-*Z* plane. (b) Same as (a) for the LDA+nonlocal Σ *Ansatz* with $k_z = 0.00$ for the hole bands fit and $k_z = 0.35$ for the electron bands fit. (c) Same as (a) for the LDA+local Σ *Ansatz* with $k_z = 0.00$ for the hole bands fit and $k_z = 0.35$ for the electron bands fit. (d) Same as (a) for the LQSGW+nonlocal Σ *Ansatz* with $k_z = 0.00$ for the hole bands fit and $k_z = 0.55$ for the electron bands fit. Red and blue dots are the δ and γ Fermi surfaces measured with ARPES in Ref. [44]. The ARPES data for fitting (b)–(d) is taken from Refs. [20,45]. See Table I for Fermi surface volumes.

We consider two different choices for the reference Hamiltonian $H(k)$. The first is the Kohn-Sham Hamiltonian obtained from density-functional theory in the local density approximation (DFT-LDA) using the WIEN2K software package [37,38]. The second is the quasiparticle Hamiltonian obtained from the linearized quasiparticle self-consistent GW method (LQSGW) using the FLAPWMBPT code [30,31]. For the localized basis set ($m\sigma$), we calculate maximally localized Wannier functions [39,40] in a wide energy window including Fe(d) and As(p) orbitals, using the WANNIER90 [41], WIEN2WANNIER [42], and COMDMFT [36] packages [see the Supplemental Material (SM) [43]]. We take the spin-orbit coupling (SOC) to be local and present only on iron atoms (see SM [43]).

We first discuss the electronic structure associated with $H(k)$, i.e., in the absence of the self-energy. In Fig. 1(a), we compare the FS of DFT-LDA to that of LQSGW. The LQSGW FS clearly displays a significant shrinking of the xz/yz dominated hole/electron pockets, α', α, and δ sheets in comparison to LDA, as pointed out in previous work [5,22,29]. This is because nonlocal electronic interactions are more prominently taken into account in the LQSGW, resulting in a repulsion of the bands between α (α') and δ. The shrinking of these FS pockets from LDA to LQSGW is also apparent from Table I, in which we compare the volumes of the different FS sheets between the two methods. The net difference between all electron and hole FS volumes is also indicated and, for both methods, adds up to zero within error bars as required by the Luttinger theorem.

The procedure for extracting the self-energy from ARPES data follows Ref. [26] for Sr_2RuO_4. From a theoretical viewpoint, the dispersions of the different branches of quasiparticles are the solutions of $\det[\omega - H(k) - \mathrm{Re}\Sigma(k,\omega)] = 0$ (neglecting the lifetime effects associated with $\mathrm{Im}\Sigma$). We

TABLE I. The net Fermi surface volumes, $V_{\mathrm{FS,total}}^{\mathrm{electron}}$-$V_{\mathrm{FS,total}}^{\mathrm{hole}}$, and Fermi surface volumes of each sheet (electrons/unit cell) in (a) the LDA, (b) the LDA+nonlocal Σ *Ansatz* ($k_z = 0.00$ for fitting of hole bands and $k_z = 0.35$ for fitting of electron bands), (c) the LDA+local Σ *Ansatz* ($k_z = 0.00$ for fitting of hole bands and $k_z = 0.35$ for fitting of electron bands), (d) the LQSGW, and (e) the LQSGW+nonlocal Σ *Ansatz* ($k_z = 0.00$ for fitting of hole bands and $k_z = 0.55$ for fitting of electron bands). 0.02–0.03 (electrons/unit cell) in the net Fermi surface volume is the numerical uncertainty.

	α'	α	β	γ	δ	Net
LDA	0.01	0.14	0.33	0.18	0.28	−0.02
LDA+nonlocal Σ	0.00	0.08	0.37	0.23	0.39	+0.17
LDA+local Σ	0.00	0.06	0.36	0.19	0.35	+0.12
LQSGW	0.00	0.08	0.35	0.20	0.21	−0.03
LQSGW+nonlocal Σ	0.00	0.05	0.36	0.20	0.26	+0.04

use the measured positions of the maximum of the momentum distribution curves (MDCs) associated with several quasiparticle bands, for a given binding energy ω, as an input to this equation which is then solved by a numerical root-finding procedure for the real part of the self-energy (for details of the procedure, see SM [43]).

To facilitate the determination of Σ, we restrict its functional form as follows. We assume that, in the local orbital basis, it is independent of the out-of-plane momentum k_z and that the off-diagonal (interorbital) matrix elements are absorbed into the renormalization of the SOC [46–48]. Two different *Ansätze* are made for the in-plane momentum dependence. (i) The self-energy components are simply assumed to be independent of momentum—we refer to this as the "local Σ *Ansatz*." (ii) The Brillouin zone is divided into two patches, centered around the Γ and M points, respectively, as illustrated in Fig. 2, and a more flexible momentum dependence is allowed which is piecewise constant in each patch. We refer

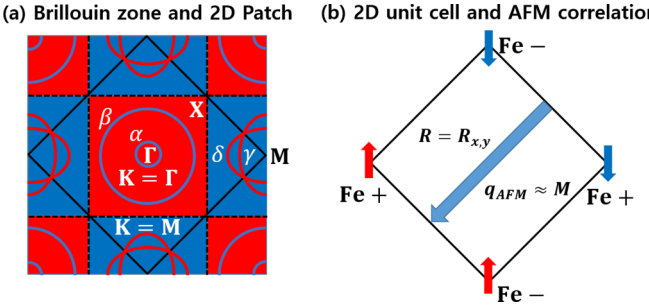

FIG. 2. (a) Patching of the Brillouin zone for the nonlocal Σ *Ansatz* of LiFeAs. The solid line delimits the principal Brillouin zone (two irons in a unit cell), and the dashed lines indicate the patching used in the nonlocal Σ *Ansatz*. The patch centered on $K = \Gamma$ (respectively, $K = M$) is colored in red (respectively, blue). Schematic Fermi surfaces are represented by colored solid lines. Hole pockets are in blue: α (inner) and β (outer). Electron pockets are in red: δ (outer) and γ (inner). (b) Two-dimensional unit cell and the momentum $q_{\mathrm{AFM}} \approx M$ associated with AFM correlations [50]. The AFM-correlated Fe moments are schematized by the blue and red arrows, with Fe+ and Fe− denoting the two Fe atoms in the unit cell.

to this *Ansatz* as the "nonlocal Σ *Ansatz*" It corresponds to a two-site dynamical cluster approximation which is a cluster extension of the DMFT [49]. These two *Ansätze* thus read (see SM for details [43])

$$\text{local } \Sigma \textit{ Ansatz}\text{: } \Sigma_m(k,\omega) = \Sigma_m(\omega), \tag{2}$$

$$\text{nonlocal } \Sigma \textit{ Ansatz}\text{: } \Sigma_m(k,\omega) = \Sigma_m(\Gamma,\omega) \text{ if } k \in \Gamma$$
$$= \Sigma_m(M,\omega) \text{ if } k \in M. \tag{3}$$

The components of the self-energy within the nonlocal Σ *Ansatz* are obtained by fitting the experimental hole bands at $K = \Gamma$ and electron bands at $K = M$ separately. We also note that this *Ansatz* is physically motivated by the AFM wave vector of spin fluctuations and corresponding Brillouin zone folding [Fig. 2(b)] [50]. We emphasize that these *Ansätze* are made for the components of the self-energy expressed in the basis of local orbitals. The transformation to the quasiparticle (band) basis is momentum dependent and leads to significant momentum dependence of the self-energy in that basis even if a DMFT *Ansatz* is made (see also Ref. [26]).

The assignment of k_z from ARPES has uncertainties [51]. In our case, experiment constraints k_z around the electron pockets are in the interval [0.3,0.7] while for the hole pockets, there is little uncertainty that the data arise from $k_z = 0$ [45] (see SM [43]). For the electron pockets, we considered two different ways to infer k_z. (i) The first is to require that the Fermi surface volume satisfies Luttinger's theorem, as obtained by a full Brillouin zone integration and assuming that the self-energy does not depend on k_z. As it turns out, for electron pockets, a unique value of $k_z \simeq 0.55$ satisfies this constraint for both *Ansätze*. (ii) The second one determines k_z by requesting that the resulting self-energy is as local as possible. This leads to $k_z = 0.35$ for the LDA+nonlocal Σ *Ansatz* and $k_z = 0.55$ for the LQSGW+nonlocal Σ *Ansatz* (see SM [43]). Note that in that case, Luttinger's theorem is violated within the LDA+nonlocal Σ *Ansatz*, while the value $k_z = 0.55$ ensures both Luttinger's theorem and maximal locality when using the LQSGW reference.

III. RESULTS

Our main results are summarized in Figs. 1(b)–1(d), 3, and Tables I and II. The full frequency dependence of the self-energies extracted from the procedure described above is displayed in Fig. S5 in the SM [43]. All results were obtained using the ARPES data of Refs. [20,45], and are displayed in Fig. 3 [52]. The low-energy behavior of the fitted self-energies is characterized by the zero-frequency (static) values $\Sigma_m(0)$, as well as the quasiparticle weights $Z_m = [1 - \frac{\partial \Sigma_m}{\partial \omega}|_{\omega=0}]^{-1}$, displayed in Table II. Comparing the values obtained within the nonlocal Σ *Ansatz* for the Γ and M BZ patches, we see that, when starting from LDA, the static components of the self-energy are spatially local to a good approximation for the xz/yz orbitals, while a higher degree of momentum dependence holds for the xy orbital. The quasiparticle weight associated with the xy orbital is found to be weakly momentum dependent, while stronger momentum dependence is found for the xz/yz orbital. This strong momentum dependence of the dynamical self-energy of the xz/yz orbitals has been discussed in Refs. [5,6,19,25] in relation to the strong coupling of the quasiparticles of the xz/yz driven α and α' holelike FS sheets to the existing AFM correlation in LiFeAs [50]. Indeed, these FS sheets are close to the AFM zone boundary. The values of the quasiparticle weights obtained here [0.15 (Γ), 0.12 (M) for xy and 0.25 (Γ), 0.16 (M) for xz/yz], are smaller than that of the computed LDA+DMFT values reported in Refs. [14,16,20] ($Z_{xy} = 0.26$ and $Z_{xz/yz} = 0.34$). They are, however, close to the values (0.17–0.19) reported by de Haas–van Alphen experiments [53].

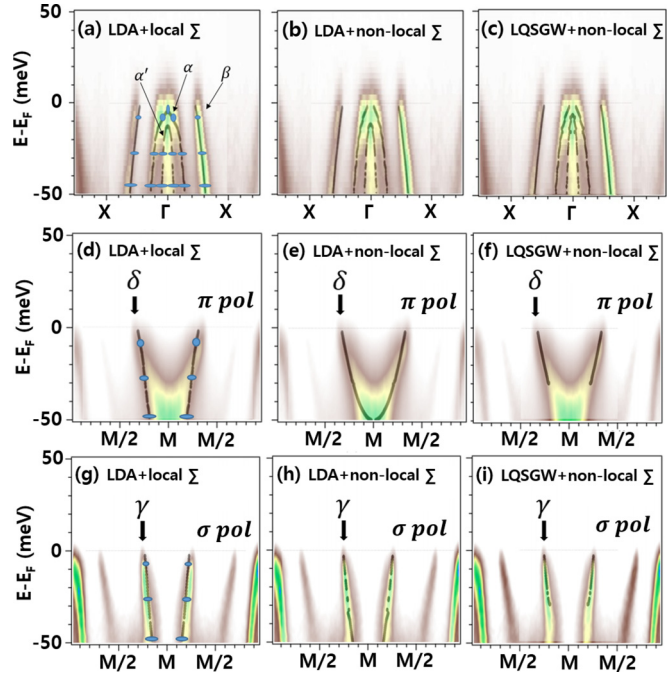

FIG. 3. Comparison between the ARPES data of Refs. [20,45] for LiFeAs (color intensity map) with different polarizations (π and σ) and the quasiparticle dispersions obtained with the different *Ansätze* discussed in the text. The results of LDA+local Σ, LDA+nonlocal Σ, and LQSGW+nonlocal Σ Ansätze are shown in panels (a), (d), and (g), (b), (e), and (h), and (c), (f), and (i), respectively. The hole pocket data are taken at $k_z = 0.00$ and the electron pockets data are taken at a value of k_z within the range of [0.3, 0.7] [20,45]. The blue ellipses are theoretical error estimates arising from the width of the MDC peak and the uncertainty in k_z. For the electron bands, $k_z = 0.55$ has been used in the fit using LQSGW as a reference, while $k_z = 0.35$ when using LDA as a reference (see main text).

Table II also displays the results obtained by using a local *Ansatz* for the self-energies. As seen there, the values of the quasiparticle weights are intermediate between the values at the Γ and M points obtained within the nonlocal *Ansatz*.

Figures 1(b) and 1(c) display how the FS is modified by self-energy effects when using LDA as a starting point. Table I reports the corresponding volume of each FS sheet. We see that both the local and nonlocal *Ansätze* lead to a violation of the Luttinger theorem, when the value $k_z = 0.35$ is used for the fitting of electron bands. This is mostly due to the large volume obtained for the δ sheet, which crosses the γ sheet at a low value of $k_z \approx 0.05$ leading to a too large electronlike contribution.

TABLE II. Zero-frequency self-energy $[\Sigma_m(K,0)]$ and quasiparticle residue $[Z_m(K)]$ extracted from ARPES data of LiFeAs [20,45], with the LDA+nonlocal Σ *Ansatz*, the LQSGW+nonlocal Σ *Ansatz*, and the LDA+local Σ *Ansatz*. We use $k_z = 0.00$ for $K = \Gamma$ (hole sheets) for both the LDA and the LQSGW references, $k_z = 0.35$ for $K = M$ (electron sheets) for the LDA reference, and $k_z = 0.55$ for $K = M$ (electron sheets), for the LQSGW reference. Error bars (total) are computed from the peak width of both in-plane k and out-of-plane k_z. (See SM for the details on the definition of the error bars [43].)

LDA+nonlocal Σ *Ansatz*				
	$\Sigma_m(\Gamma,0)$ (eV)	$Z_m(\Gamma)$	$\Sigma_m(M,0)$ (eV)	$Z_m(M)$
xy	0.029±0.025	0.15±0.01	-0.130 ± 0.062	0.12±0.01
xz/yz	-0.083 ± 0.040	0.25±0.13	-0.113 ± 0.026	0.16±0.03
LDA+local Σ *Ansatz*				
	$\Sigma_m(0)$ (eV)		Z_m	
xy	0.023		0.14	
xz/yz	−0.112		0.17	
LQSGW+nonlocal Σ *Ansatz*				
	$\Sigma_m(\Gamma,0)$ (eV)	$Z_m(\Gamma)$	$\Sigma_m(M,0)$ (eV)	$Z_m(M)$
xy	0.002±0.014	0.21±0.01	0.044±0.036	0.18±0.01
xz/yz	-0.027 ± 0.003	0.38±0.01	-0.051 ± 0.114	0.30±0.04

We now turn to the results of the self-energy obtained by using LQSGW for the reference Hamiltonian, using $k_z = 0.55$ in this case when fitting the electron bands around M. The results in Table II clearly show that the fitted values of both $\Sigma_m(0)$ and Z_m are quite momentum independent (spatially local) within the determined error bars. Some slight momentum dependence of $Z_{xz/yz}$ is found, however (∼0.38 at the Γ point vs ∼0.30 at the M point), close to the limit set by error bars (see Fig. S5 of the SM [43] for the full frequency dependence of the extracted self-energies). Furthermore the Luttinger theorem is now well obeyed (Table I). This is due in particular to the much smaller inflation of the volume of the γ and δ sheets by self-energy effects, in comparison to the LDA starting point. Correspondingly, the crossing point between the γ and δ sheets occurs at a larger value of k_z [Fig. 1(d)].

Comparing to available experimental data, we see that the LQSGW reference combined with a quasilocal self-energy provides (i) a good description of the k_z-dependent hole band (α', α, and β) dispersions in comparison to the ARPES data of Refs. [20,54] (see SM [43] for comparison), (ii) a good description of the k_z-dependent γ FS in ARPES of Refs. [44,55], and (iii) a qualitative description of the k_z-dependent δ FS in ARPES with correct k_z for the crossing of the δ and γ FSs and somewhat larger curvature of the δ FS near the momentum of A of Refs. [44,45]. Figure 1(d) implies that for electron bands, the overall amplitude of k_z-dependent variation of the δ and γ FSs in the LQSGW+ fit is consistent with the ARPES data of Ref. [44].

We compare in Figs. 3(a)–3(c) the experimental ARPES intensity to the fitted hole bands of LiFeAs using the different starting points $H(k)$ and *Ansatz* for Σ. For the xy dominant β band, all schemes compare well with ARPES. In contrast, we observe some differences between the different *Ansätze* (comparable to error bars) for the position of the top of the α band with dominant xz/yz character. The LDA+local Σ *Ansatz* leads to a lower energy than the LDA+nonlocal Σ *Ansatz* and the LQSGW+nonlocal Σ *Ansatz*. The splitting of the states with xz/yz character at the Γ point is controlled by the SOC and given by $\lambda Z_{xz/yz}$ [46]. Its experimental value is 9.5–11.4 meV [56,57]. The values of λ in LDA and LQSGW are 50 and 25 meV, respectively, which when multiplied by the extracted Z's from Table II, indeed leads to values close to 10 meV in both cases (see SM for details on the effect of SOC in LiFeAs [43]).

We now turn to the electron bands in Figs. 3(d)–3(i). Along the Γ-M direction, the γ band has almost pure xy character, and is seen in σ polarized ARPES. This γ band is well described by both the nonlocal *Ansatz* and the local *Ansatz* within both references (LDA and LQSGW) [see Figs. 3(g)–3(i)]. For the xz/yz dominant δ band, the LDA+nonlocal Σ *Ansatz* and the LQSGW+nonlocal Σ *Ansatz* yield quasiparticle spectra which are consistent with ARPES within error bars as shown in Figs. 3(e) and 3(f). However, differences between the fits are seen for the xz/yz driven δ band with the LDA+local Σ *Ansatz* having a steeper dispersion and a lower bottom than the nonlocal Σ *Ansatz*, as seen in Figs. 3(d)–3(f). Also, as noted in Table I and Figs. 1(b) and 1(c), this fit violates the Luttinger theorem.

In summary, our analysis demonstrates that an LQSGW reference [29,36,58] in combination with quite local self-energies provides a description of the quasiparticle dispersions of LiFeAs in good agreement with experiments. The strong dispersion along k_z of the α and δ FS sheets, unique to the 111 compounds, is also well described, although the latter is slightly overestimated. Hence, correlation effects can be decomposed into nonlocal, frequency-independent contributions captured by the LQSGW and dynamical frequency-dependent contributions that are spatially local to a good approximation. In contrast, when using LDA as a reference, the extracted self-energy is spatially nonlocal and, when taken to be k_z independent, leads to an overestimation of the volume of the FS δ sheet and a corresponding violation of the Luttinger theorem. We emphasize that, in contrast to theories attributing nonlocality to AFM spin fluctuations, the nonlocality in the LQSGW approach originates from the charge sector.

We finally turn to transport measurements, as reported in Ref. [59], and investigate whether our LQSGW+local Σ analysis is consistent with those data. Using the occupancies of the different FS sheets obtained above, we use the experimental data for the resistivity and Hall effect to obtain the scattering rates associated with each orbital component, as a function of temperature, under the assumption that they are spatially local. The conclusion of this analysis (see details in SM [43]) is that the xy orbital is found to have a larger scattering rate than the xz/yz one, and that it undergoes a clear crossover at $T \sim 150$ K between a high-T incoherent regime to a low-T coherent one. This is consistent with the LQSGW+local Σ finding that the xy orbital is the more correlated one. At low T both scattering rates are found to have a Fermi liquid T^2 behavior. As a consistency check, we also obtain satisfactory agreement with the magnetoresistance data. Let us emphasize that, in contrast, studies emphasizing nonlocality due to low-energy AFM fluctuations yield a non-Fermi-liquid scattering rate of the xz/yz orbital which is larger than that of xy [5,6].

Several authors have pointed at some discrepancies between experimental data and the predictions of LDA+DMFT, which is usually interpreted as a failure of the DMFT to take into account nonlocal effects [5,6,24,25,60]. Here, based on a direct analysis of ARPES experimental data, we presented a very different picture, consistent with the electronic structure+DMFT conceptual framework. We have shown that when we start from the LQSGW reference Hamiltonian, the low-energy self-energy is spatially local, satisfies Luttinger's theorem, describes available experimental data well, and therefore is an attractive platform to study how superconductivity emerges at lower temperatures [9,11–13,15,18].

Note added in proof. We became aware of a related work by T. Gorni *et al.* [61], which shows that the approximation of the electronic correlations, separated into static nonlocal contributions and dynamical local contributions, has a validity in the description of the electronic structure of another iron-based superconductor, FeSe, supporting the general conclusion of this paper.

ACKNOWLEDGMENTS

We acknowledge useful discussions with Andrea Damascelli and Ryan Day (who also kindly shared their unpublished ARPES data) as well as with Roser Valenti. This work was supported by the DOE CMS program (M.K. and G.K.). S.C. was supported by the U.S. Department of Energy, Office of Science, Basic Energy Sciences as a part of the Computational Materials Science Program. For the LQSGW calculation, we used resources of the National Energy Research Scientific Computing Center (NERSC), a U.S. Department of Energy Office of Science User Facility operated under Contract No. DE-AC02-05CH11231. H.M. was supported by the Laboratory Directed Research and Development Program of Oak Ridge National Laboratory, managed by UT-Battelle, LLC, under Contract No. DE-AC05-00OR22725 for the U.S. Department of Energy. A.G. acknowledges the support of the European Research Council (ERC-319286-QMAC). The Flatiron Institute is a division of the Simons Foundation.

[1] Y. Kamihara, H. Hiramatsu, M. Hirano, R. Kawamura, H. Yanagi, T. Kamiya, and H. Hosono, J. Am. Chem. Soc. **128**, 10012 (2006).
[2] I. I. Mazin, D. J. Singh, M. D. Johannes, and M. H. Du, Phys. Rev. Lett. **101**, 057003 (2008).
[3] K. Kuroki, S. Onari, R. Arita, H. Usui, Y. Tanaka, H. Kontani, and H. Aoki, Phys. Rev. Lett. **101**, 087004 (2008).
[4] A. V. Chubukov, D. V. Efremov, and I. Eremin, Phys. Rev. B **78**, 134512 (2008).
[5] K. Zantout, S. Backes, and R. Valentí, Phys. Rev. Lett. **123**, 256401 (2019).
[6] J. Fink, J. Nayak, E. D. L. Rienks, J. Bannies, S. Wurmehl, S. Aswartham, I. Morozov, R. Kappenberger, M. A. ElGhazali, L. Craco, H. Rosner, C. Felser, and B. Büchner, Phys. Rev. B **99**, 245156 (2019).
[7] P. Dai, Rev. Mod. Phys. **87**, 855 (2015).
[8] L. Fanfarillo, E. Cappelluti, C. Castellani, and L. Benfatto, Phys. Rev. Lett. **109**, 096402 (2012).
[9] K. Umezawa, Y. Li, H. Miao, K. Nakayama, Z.-H. Liu, P. Richard, T. Sato, J. B. He, D.-M. Wang, G. F. Chen, H. Ding, T. Takahashi, and S.-C. Wang, Phys. Rev. Lett. **108**, 037002 (2012).
[10] S. Hoshino and P. Werner, Phys. Rev. Lett. **115**, 247001 (2015).
[11] H. Miao, W. H. Brito, Z. P. Yin, R. D. Zhong, G. D. Gu, P. D. Johnson, M. P. M. Dean, S. Choi, G. Kotliar, W. Ku, X. C. Wang, C. Q. Jin, S.-F. Wu, T. Qian, and H. Ding, Phys. Rev. B **98**, 020502(R) (2018).
[12] T.-H. Lee, A. Chubukov, H. Miao, and G. Kotliar, Phys. Rev. Lett. **121**, 187003 (2018).
[13] P. Coleman, Y. Komijani, and E. J. König, Phys. Rev. Lett. **125**, 077001 (2020).
[14] Z. Yin, K. Haule, and G. Kotliar, Nat. Mater. **10**, 932 (2011).
[15] H. Miao, P. Richard, Y. Tanaka, K. Nakayama, T. Qian, K. Umezawa, T. Sato, Y.-M. Xu, Y. B. Shi, N. Xu, X.-P. Wang, P. Zhang, H.-B. Yang, Z.-J. Xu, J. S. Wen, G.-D. Gu, X. Dai, J.-P. Hu, T. Takahashi, and H. Ding, Phys. Rev. B **85**, 094506 (2012).
[16] G. Lee, H. S. Ji, Y. Kim, C. Kim, K. Haule, G. Kotliar, B. Lee, S. Khim, K. H. Kim, K. S. Kim, K.-S. Kim, and J. H. Shim, Phys. Rev. Lett. **109**, 177001 (2012).
[17] P. Werner, M. Casula, T. Miyake, F. Aryasetiawan, A. J. Millis, and S. Biermann, Nat. Phys. **8**, 331 (2012).
[18] Z. P. Yin, K. Haule, and G. Kotliar, Nat. Phys. **10**, 845 (2014).
[19] H. Miao, T. Qian, X. Shi, P. Richard, T. K. Kim, M. Hoesch, L. Y. Xing, X.-C. Wang, C.-Q. Jin, J.-P. Hu, and H. Ding, Nat. Commun. **6**, 6056 (2015).
[20] H. Miao, Z. P. Yin, S. F. Wu, J. M. Li, J. Ma, B.-Q. Lv, X. P. Wang, T. Qian, P. Richard, L.-Y. Xing, X.-C. Wang, C. Q. Jin, K. Haule, G. Kotliar, and H. Ding, Phys. Rev. B **94**, 201109(R) (2016).
[21] P. Sémon, K. Haule, and G. Kotliar, Phys. Rev. B **95**, 195115 (2017).
[22] J. M. Tomczak, M. van Schilfgaarde, and G. Kotliar, Phys. Rev. Lett. **109**, 237010 (2012).
[23] J. Ferber, K. Foyevtsova, R. Valentí, and H. O. Jeschke, Phys. Rev. B **85**, 094505 (2012).
[24] L. Ortenzi, E. Cappelluti, L. Benfatto, and L. Pietronero, Phys. Rev. Lett. **103**, 046404 (2009).
[25] S. Bhattacharyya, K. Björnson, K. Zantout, D. Steffensen, L. Fanfarillo, A. Kreisel, R. Valentí, B. M. Andersen, and P. J. Hirschfeld, Phys. Rev. B **102**, 035109 (2020).
[26] A. Tamai, M. Zingl, E. Rozbicki, E. Cappelli, S. Riccò, A. de la Torre, S. McKeown Walker, F. Y. Bruno, P. D. C. King, W. Meevasana, M. Shi, M. Radović, N. C. Plumb, A. S. Gibbs, A. P. Mackenzie, C. Berthod, H. U. R. Strand, M. Kim, A. Georges, and F. Baumberger, Phys. Rev. X **9**, 021048 (2019).
[27] J. H. Tapp, Z. Tang, B. Lv, K. Sasmal, B. Lorenz, P. C. W. Chu, and A. M. Guloy, Phys. Rev. B **78**, 060505(R) (2008).
[28] T. Mertz, K. Zantout, and R. Valentí, Phys. Rev. B **98**, 235105 (2018).

[29] J. M. Tomczak, J. Phys.: Conf. Ser. **592**, 012055 (2015).

[30] A. L. Kutepov, V. S. Oudovenko, and G. Kotliar, Comput. Phys. Commun. **219**, 407 (2017).

[31] A. Kutepov, K. Haule, S. Y. Savrasov, and G. Kotliar, Phys. Rev. B **85**, 155129 (2012).

[32] A. Georges, G. Kotliar, W. Krauth, and M. J. Rozenberg, Rev. Mod. Phys. **68**, 13 (1996).

[33] G. Kotliar, S. Y. Savrasov, K. Haule, V. S. Oudovenko, O. Parcollet, and C. A. Marianetti, Rev. Mod. Phys. **78**, 865 (2006).

[34] M. Qazilbash, J. Hamlin, R. Baumbach, L. Zhang, D. J. Singh, M. Maple, and D. Basov, Nat. Phys. **5**, 647 (2009).

[35] L. de' Medici, G. Giovannetti, and M. Capone, Phys. Rev. Lett. **112**, 177001 (2014).

[36] S. Choi, P. Semon, B. Kang, A. Kutepov, and G. Kotliar, Comput. Phys. Commun. **244**, 277 (2019).

[37] P. Blaha, K. Schwarz, G. K. H. Madsen, D. Kvasnicka, and J. Luitz, *WIEN2K: An Augmented Plane Wave and Local Orbitals Program for Calculating Crystal Properties* (Vienna University of Technology, Austria, 2001).

[38] P. Blaha, K. Schwarz, F. Tran, R. Laskowski, G. K. Madsen, and L. D. Marks, J. Chem. Phys. **152**, 074101 (2020).

[39] I. Souza, N. Marzari, and D. Vanderbilt, Phys. Rev. B **65**, 035109 (2001).

[40] N. Marzari and D. Vanderbilt, Phys. Rev. B **56**, 12847 (1997).

[41] A. A. Mostofi, J. R. Yates, Y.-S. Lee, I. Souza, D. Vanderbilt, and N. Marzari, Comput. Phys. Commun. **178**, 685 (2008).

[42] J. Kuneš, R. Arita, P. Wissgott, A. Toschi, H. Ikeda, and K. Held, Comput. Phys. Commun. **181**, 1888 (2010).

[43] See Supplemental Material at http://link.aps.org/supplemental/10.1103/PhysRevB.103.155107 for (i) information on the construction of $H(k)$ with maximally localized Wannier function for DFT-LDA and LQSGW, (ii) details of the microscopic calculations include SOC, (iii) k_z-dependent electron band dispersions of $H(k)$, (iv) details of the method for the extraction of the self-energy including error bars, (v) comparison of the quality of the present LQSGW+nonlocal Σ fit to the published ARPES data, showing that the fitting of the hole pockets leads to a good description of the published data for $k_z = 0.00$ [20] and for other values of k_z [54], (vi) self-energy depending on the assigned k_z value for electron pockets and corresponding Fermi surface volumes for the Luttinger's theorem, (vii) frequency dependency of the dynamical self-energy, and (viii) analysis of the transport data of Ref. [59] and discussions of the extracted scattering rate from the transport data.

[44] V. Brouet, D. LeBoeuf, P.-H. Lin, J. Mansart, A. Taleb-Ibrahimi, P. Le Fèvre, F. Bertran, A. Forget, and D. Colson, Phys. Rev. B **93**, 085137 (2016).

[45] Hu Miao (unpublished).

[46] M. Kim, J. Mravlje, M. Ferrero, O. Parcollet, and A. Georges, Phys. Rev. Lett. **120**, 126401 (2018).

[47] N.-O. Linden, M. Zingl, C. Hubig, O. Parcollet, and U. Schollwöck, Phys. Rev. B **101**, 041101(R) (2020).

[48] A. Horvat, R. Zitko, and J. Mravlje, Phys. Rev. B **96**, 085122 (2017).

[49] T. A. Maier, M. Jarrell, T. Pruschke, and M. Hettler, Rev. Mod. Phys. **77**, 1027 (2005).

[50] N. Qureshi, P. Steffens, Y. Drees, A. C. Komarek, D. Lamago, Y. Sidis, L. Harnagea, H. J. Grafe, S. Wurmehl, B. Buchner, and M. Braden, Phys. Rev. Lett. **108**, 117001 (2012).

[51] A. Damascelli, Phys. Scr. **2004**, 61 (2004).

[52] The ARPES data has been measured at 20 K, which is slightly above the superconducting transition temperature (18 K) of LiFeAs [27].

[53] C. Putzke, A. I. Coldea, I. Guillamon, D. Vignolles, A. McCollam, D. LeBoeuf, M. D. Watson, I. I. Mazin, S. Kasahara, T. Terashima, T. Shibauchi, Y. Matsuda, and A. Carrington, Phys. Rev. Lett. **108**, 047002 (2012).

[54] Z. Wang, P. Zhang, G. Xu, L. K. Zeng, H. Miao, X. Xu, T. Qian, H. Weng, P. Richard, A. V. Fedorov, H. Ding, X. Dai, and Z. Fang, Phys. Rev. B **92**, 115119 (2015).

[55] T. Hajiri, T. Ito, R. Niwa, M. Matsunami, B. H. Min, Y. S. Kwon, and S. Kimura, Phys. Rev. B **85**, 094509 (2012).

[56] S. Borisenko, D. Evtushinsky, Z.-H. Liu, I. Morozov, R. Kappenberger, S. Wurmehl, B. Büchner, A. Yaresko, T. Kim, M. Hoesch *et al.*, Nat. Phys. **12**, 311 (2016).

[57] R. P. Day, G. Levy, M. Michiardi, B. Zwartsenberg, M. Zonno, F. Ji, E. Razzoli, F. Boschini, S. Chi, R. Liang, P. K. Das, I. Vobornik, J. Fujii, W. N. Hardy, D. A. Bonn, I. S. Elfimov, and A. Damascelli, Phys. Rev. Lett. **121**, 076401 (2018).

[58] S. Choi, A. Kutepov, K. Haule, M. van Schilfgaarde, and G. Kotliar, npj Quantum Mater. **1**, 16001 (2016).

[59] F. Rullier-Albenque, D. Colson, A. Forget, and H. Alloul, Phys. Rev. Lett. **109**, 187005 (2012).

[60] S.V. Borisenko, V. B. Zabolotnyy, D. V. Evtushinsky, T. K. Kim, I. V. Morozov, A. N. Yaresko, A. A. Kordyuk, G. Behr, A. Vasiliev, R. Follath, and B. Buchner, Phys. Rev. Lett. **105**, 067002 (2010).

[61] T. Gorni, P. V. Arribi, M. Casula, and L. de' Medici, arXiv:2101.01692 (2021).